Quaternary Research

doi:10.1017/qua.2019.78

Chronological and geomorphological approach to the Holocene tephras from Tafí and Santa María valleys, NW Argentina

María M. Sampietro-Vattuone[a,b*], Walter A. Báez[c,d], José L. Peña-Monné[e], Alfonso Sola[c,d]

[a]Laboratorio de Geoarqueología, Facultad de Ciencias Naturales e Instituto Miguel Lillo, Universidad Nacional de Tucumán, San Miguel de Tucumán, Tucumán, Argentina
[b]CONICET, Tucumán, Argentina
[c]Cátedra de Petrología Ígnea y Metamórfica – Escuela de Geología – Facultad de Ciencias Naturales – Universidad Nacional de Salta, Salta, Argentina
[d]Instituto de Bio y Geociencias del NOA (IBIGEO) – CONICET, Salta, Argentina
[e]Departamento de Geografía y Ordenación del Territorio and IUCA, Universidad de Zaragoza, Zaragoza, Spain
*Corresponding author e-mail address: sampietro@tucbbs.com.ar (M.M. Sampietro-Vattuone).

(Received April 22, 2019; Accepted November 7, 2019)

Abstract

A comprehensive morphostratigraphic and chronological study of the complete set of Holocene tephras from Tafí and Santa María valleys (northwestern Argentina), including analyses of compositional characteristics, is presented. Five ash tephras are recognized: V0 (El Rincón), V1a (Carreras 1a ash), V1b (Carreras 1b ash), V2a (Carreras 2 ash), and V2b (El Paso 3 ash). Two of them (V1b and V2b) are described for the first time in the study area. The new ^{14}C and accelerator mass spectrometry ages presented, along with the previously published information, allows for the establishment of a chronological framework. The V0 tephra was deposited in the Early Holocene (about 10,000 yr BP), V1a and V1b were deposited in the Middle Holocene (about 4200 and 3500 yr BP, respectively), and V2a and V2b were deposited in the Late Holocene (after about 800 yr BP). The mineralogical, textural, and geochemical characterizations of the five tephras suggest that their tephra provenance was mainly from the back-arc region. However, the determination of the exact source of each tephra requires more accurate high-resolution tephrochronological studies. At least five major eruptions affected the Tafí and Santa María valleys in the last 10,000 yr.

Keywords: Tephrostratigraphy; Explosive volcanism; Volcanic hazard; Central Volcanic Zone

INTRODUCTION

Along the southern sector of the Central Volcanic Zone of the Andes (between 24° and 27° latitude), a magmatic arc of north–south general orientation, with prolongations toward the back-arc following the regional northwest–southeast tectonic lineaments, has developed since the Neogene (Kay and Coira, 2009; Petrinovic et al., 2017). Recent volcanic activity in this region is mainly associated with andesitic-dacitic stratovolcanoes along the main arc, some of which are considered potentially active, although most are poorly known (Siebert et al., 2010; Grosse et al., 2018). Very few of these stratovolcanoes have recorded historical activity, and only Lascar volcano has registered regular eruptions in recent decades (Gardeweg et al., 1998). In addition, the most recent eruptive history of these volcanoes is characterized by the development of effusive or small explosive eruptions (e.g., Grosse et al., 2018), except for the Tres Cruces volcano, which had important explosive activity during the Holocene (Gardeweg et al., 2000). Besides, recent studies have revealed the importance of back-arc volcanism in this region during the Holocene (Báez et al., 2015; Báez et al., 2017; Bertin et al., 2018). Especially relevant is the Cerro Blanco Volcanic Complex, defined as the youngest (middle Pleistocene–Holocene) collapse caldera system in the southern Central Andes. Over the past 100,000 yr, this complex has experienced at least two large-scale eruptions with Volcanic Explosivity Index (VEI) ≥6 (Báez et al., 2015; Fernández-Turiel et al., 2019). Particularly, the caldera-forming Cerro Blanco eruption constitutes one of the greatest Holocene volcanic events in the Central Andes (Báez et al., 2015; Fernández-Turiel et al., 2019). Other high-silica volcanic centers located in the back-arc, such as Cuero de Purulla volcano, have been proposed as plausible candidates for the source of large explosive eruptions during the upper Pleistocene–Holocene (Báez, 2014; Fernández-Turiel et al., 2019).

Cite this article: Sampietro-Vattuone, M. M., Báez, W. A., Peña-Monné, J. L., Sola, A. 2020. Chronological and geomorphological approach to the Holocene tephras from Tafí and Santa María valleys, NW Argentina. *Quaternary Research* 94, 14–30. https://doi.org/10.1017/qua.2019.78

Because of the influence of the subtropical westerly jet in the middle and upper troposphere (Garreaud et al., 2009), the explosive volcanic activity of the main arc, as well as that of the back-arc, tends to disperse the tephras toward the east. Thus, in the intermontane valleys located eastward of the Puna, such as Santa María and Tafí valleys, a record of the Holocene large explosive eruptions is preserved. Previous works have addressed the tephrochronology of this region. Strecker (1987) identified some tephra layers in the Santa María and Tafí valleys and used them to establish the age of Pleistocene accumulations.

Later, tephra levels were used to determine the age of large Holocene landslides produced downstream of the confluence of the Santa María and Calchaquí Rivers (Hermanns et al., 2000; Trauth et al., 2000). Other studies have also correlated the tephras from Santa María and Tafí valleys (May et al., 2011). The most comprehensive study about northwestern Argentina tephrochronology shows a unified analysis of all Quaternary layers recorded in the region until 2008 (Hermann and Schellenberger, 2008). Their study describes and dates 10 well-defined tephra layers, 5 of which belong to the Holocene (see further comments on them in the "Discussion"). In addition, Fernández-Turiel et al. (2012, 2013, 2015, 2019) studied the ash dispersion of the tephras of the Cerro Blanco Volcanic Complex, took samples from proximal and distal deposits, and dated them to 4290 ± 40 ^{14}C yr BP. Proximal deposits of the same volcanic complex were also studied in depth by Báez (2014) and Báez et al. (2015). Furthermore, Sampietro-Vattuone and Peña-Monné (2016), Peña Monné and Sampietro Vattuone (2016b), and Sampietro-Vattuone et al. (2016) reported three tephra levels in Tafí valley as reference geomorphological layers, named V0, V1, and V2.

Despite previous studies, no data are available about tephra associations within Holocene deposits (slopes, debris flows, and alluvial accumulations) or soils. These tephras have never been analyzed for their evolutionary value in their geomorphological and geoarchaeological context. Moreover, not all tephras were previously described. In this context, the aim of this article is to present a comprehensive study of the complete set of Holocene tephras from Tafí and Santa María valleys (Fig. 1), their morphostratigraphic and geoarchaeological contexts, chronology, and some compositional characteristics, including a review of the previous data.

Regional settings

The Santa María and Tafí valleys are located in northwestern Argentina, including three Argentinean provinces (Tucumán, Catamarca, and Salta). Both valleys are part of the northern sector of Sierras Pampeanas and are located about 300 km east of the Central Volcanic Zone of the Andean Ranges. They are two tectonic depressions bordered by the Sierra de Aconquija (4600 m), Cumbres Calchaquíes (4177 m), and Sierra de Quilmes (5468 m) (Fig. 1). Geologically, the surrounding mountains are composed of granite and metamorphic rocks of Precambrian–Lower Paleozoic ages (Ruiz Huidobro, 1972; Toselli et al., 1978; Galván, 1981). In the Santa Maria valley, Upper Cretaceous–Neogene sediments are also visible (Salta and Santa María Groups; Bossi et al., 2001), whereas Paleogene deposits are present in Tafí valley (González, 1997).

The climate is semiarid in Santa María valley, with an annual rainfall of 200 mm, and the vegetation is xerophitic with bushes (*Larrea divaricata* and *L. cuneifolia*) and carob trees (*Prosopis* sp.) on the valley floor. Although Tafí valley is also semiarid, annual rainfall reaches 500 mm, so grasslands dominate the landscape with development of small

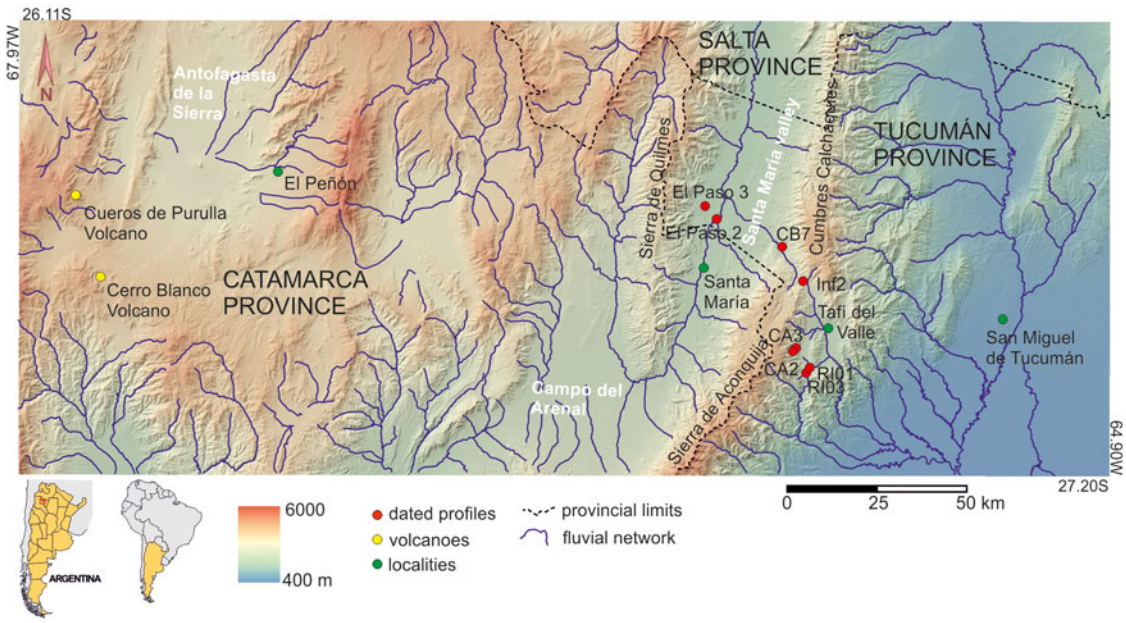

Figure 1. (color online) Study area and location of dated profiles.

https://doi.org/10.1017/qua.2019.78 Published online by Cambridge University Press

forests (*Alnus acuminata* and *Polylepis australis*) in the ravines and *quebradas* (Perea, 1995).

In addition to the geomorphological analysis of Strecker (1987) performed in Santa María valley, some studies have focused on large Holocene landslides and a paleolake formation related to them (Hermanns et al., 2006, 2011). Recent geomorphological research was performed by Sampietro Vattuone and Neder (2011), Peña-Monné et al. (2015, 2016), Peña-Monné and Sampietro-Vattuone (2016a, 2018a, 2018b), and Sampietro-Vattuone et al. (2017, 2018a). These studies focused on the Quaternary and present fluvial dynamics, the Holocene eolian activity, and the regional geomorphological evolution.

There is a long tradition of geomorphological studies at Tafí valley (Sayago and Collantes, 1991; Sayago et al., 1998; Collantes, 2001, 2007). However, recent studies have notably changed the geomorphological information, departing from wider data gathering and interpretation, where volcanic ash layers played an important role (Peña Monné and Sampietro Vattuone, 2016b; Sampietro-Vattuone and Peña-Monné, 2016; Sampietro Vattuone et al., 2016; Sampietro-Vattuone et al., 2018b). Thus, the new geomorphological cartography (Sampietro-Vattuone and Peña-Monné, 2019) and fieldwork have made it possible to establish the Holocene evolutionary model of the region. This model establishes the existence of four Holocene aggradation units separated by incision phases. Figure 2a shows a curve with estimated aggradation/degradation rates along these units. It also represents the position of the up to now three known tephras (V0, V1, and V2) and preliminary chronologies. Figure 2b shows a synthetic cross section of the sedimentary record produced by the geomorphological evolution of the area, including all paleoenvironmental features such as soil development. Radiocarbon dating indicate that the earliest evolutionary unit, named H1, spans from ca. 13,000 to 4200 yr BP and is mainly represented in the landscape by slope deposits. During the earliest times of this unit (H1A), wetter environments were dominant. A gradual shift to harsher conditions

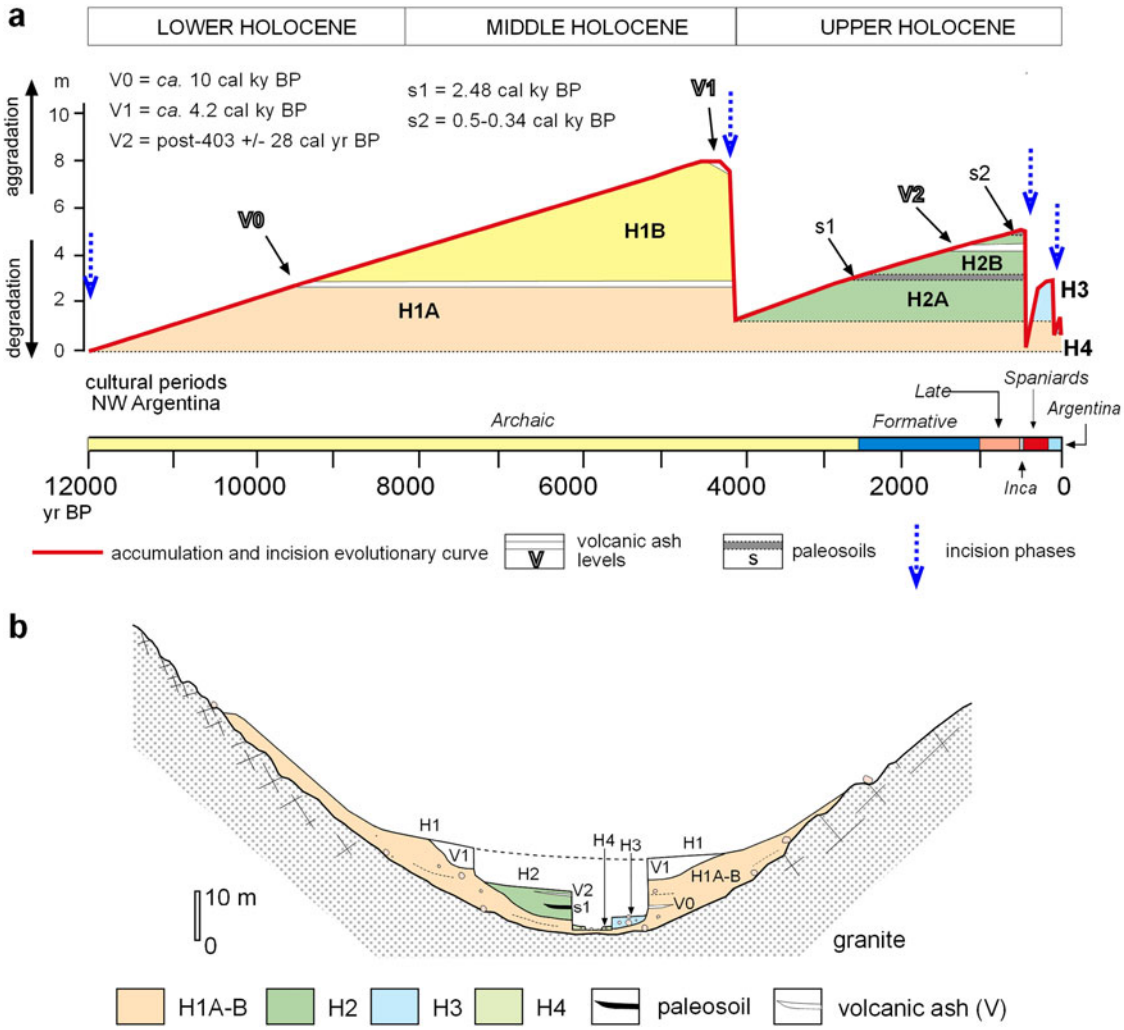

Figure 2. (color online) (a) Holocene evolutionary model of Santa María and Tafí valleys with V0, V1, and V2 relative tephra positions; the curve represents aggradation/degradation rates during the different units. (b) Synthetic cross section representative of the relative position of the different aggradative units and the tephra levels in ravines.

https://doi.org/10.1017/qua.2019.78 Published online by Cambridge University Press

was also observed at the end of the period (H1B). There are two tephra layers related to H1 unit, named V0 and V1 (Fig. 2). The H1 unit was followed by the development of a Late Holocene accumulative unit (H2) dated between ca. 4200 and 600 yr BP. It is represented in the landscape by slopes, alluvial terraces, and alluvial fan deposits. This accumulation was formed at the beginning under wetter conditions, allowing the formation of a soil (*s1*) (Fig. 2). The H2 unit also includes features that have been attributed to general environmental degradation caused by intense human impact on the landscape after soil formation (Sampietro Vattuone et al., 2018b). On top of this unit, there is another tephra named V2 overlain by a soil (*s2*) (Fig. 2). Smaller deposits from the later H3 and H4 units are recognizable in the inner sections of the incision that cuts through the previous deposits (Fig. 2b). These units were dated from after ca. 600 yr PB to the present time, and they include the Little Ice Age and the present warm period (Fig. 2).

METHODS

We first made a detailed geomorphological map of the study area following Peña Monné's proposal (1997) and a subsequent systematic field survey recording about 150 stratigraphic profiles to define the morphosedimentary units of different genesis (fluvial deposits, alluvial fans, and slopes). Transversal and longitudinal profiles were also made to know the relative position of the tephras. Several tephras were described and sampled in their morphostratigraphic context (considering stratigraphic and geomorphological positions), and 91 samples were analyzed. We selected mostly primary tephras or scarcely reworked tephras for the analyses, by considering the layer thickness, color, homogeneity, contacts with under- and overlying deposits, and the lack of internal structures, bioturbation features, and inclusions. Simultaneously, we created a complete record of erosive features associated with tephra deposits. Tephra ages were determined indirectly by ^{14}C radiometric dating of over- or underlying peats, organic matter from soils, and archaeological charcoals, together with ceramic potsherds by thermoluminiscence. Radiocarbon ages were calibrated with Oxcal v. 4.3 over the SHCal 13 curve and expressed with two sigmas.

To make a qualitative compositional and textural characterization of the tephras, bulk samples were described under binocular magnifying glass. For a better mineralogical characterization, the samples were sieved to concentrate the material retained in a #60 size mesh screen (250 μm). Further morphological analyses were based on scanning electron microscopy (SEM) images. For SEM analyses, a JEOL scanning microscope (LASEM–Universidad Nacional de Salta) was used at an acceleration voltage of 15 kV, and the samples were mounted on a holder and coated with Au.

The tephras were geochemically characterized by means of 86 bulk-rock analyses using portable X-ray fluorescence (pXRF), as proposed by Sola et al. (2016). Data were acquired using a handheld Thermo Scientific Niton XL3t GOLDD XRF spectrometer with a 50 kV, 200 μA Ag Anode X-ray tube, mounted on a test stand. Most pXRF spectrometers offer analyses in three modes: (1) test all GEO mode, where the expected elemental concentration is unknown by the user; (2) mining mode, where the expected elemental concentration is >1%; and (3) soil mode, where the expected concentration is <1%. All analyses were carried out in soil mode on powder material. All samples were analyzed with 30 s dwell times for main and low filters, and 40 s for the high filter, for a total of 70 s per analysis, following the values recommended by Knight et al. (2013): >30 s and <70 s per filter. The elements to make the geochemical characterization (Sr, Rb, Zr, Cr, Zn, Pb, U, and Th) were selected based on the detection limits according to the rock type and relatively low 2σ errors.

RESULTS

Field descriptions, morphostratigraphic analysis, and geochronology

The complementary work of geomorphological mapping and field survey made it possible to recognize five tephra layers included in several morphostratigraphic profiles. These profiles were recorded from geomorphological units of different ages and genesis. The tephra levels were not continuous across the entire study area (note that we prospected two neighboring valleys), so stratigraphic positions were recorded in order to reconstruct a wide and confident morphostratigraphic context. The five tephras appear interbedded in several morphosedimentary contexts, from which we inferred their ages. Although about 150 profiles were described during the fieldwork, only seven were selected for this study (Figs. 1, 3, and 4), considering the presence of overlying tephra layers, absolute chronological data, and morphostratigraphic representativeness. We selected the RI01 profile (Fig. 3a) for the oldest tephra (V0) and RI03 (Fig. 3d) for V1a and V1b tephras. Besides, V1a, V1b, and V2 tephras were described and dated in CA2 and CA3 profiles (Fig. 3b and c), while V2 was described and dated in Inf2, El Paso 2, and CB7 profiles (Fig. 4, Table 1). After the stratigraphic records it was clear that the three tephras preliminary established were in fact five.

The cross sections recorded in several valleys contribute to improving the knowledge of the relative positions of the tephras (Fig. 2b). Several factors conditioned their positions and thickness. First, topography and wind circulation favored tephra accumulation in some specific locations (i.e., at present some deposits in the ravines reach 8 m in thickness), whereas there is no tephra accumulation in several outcrops because of environmental erosion. Another important factor related to tephra visibility is the ravine depth, with incisions in some cases reaching the oldest deposits (Fig. 2b). In all cases, tephra visibility is conditioned not only by its relative present position but also by the processes the tephra underwent during the geomorphological evolution of the area.

Tephra V0 never appears on the topographic surface. It is only visible in the incision scarps, rendering it an excellent

https://doi.org/10.1017/qua.2019.78 Published online by Cambridge University Press

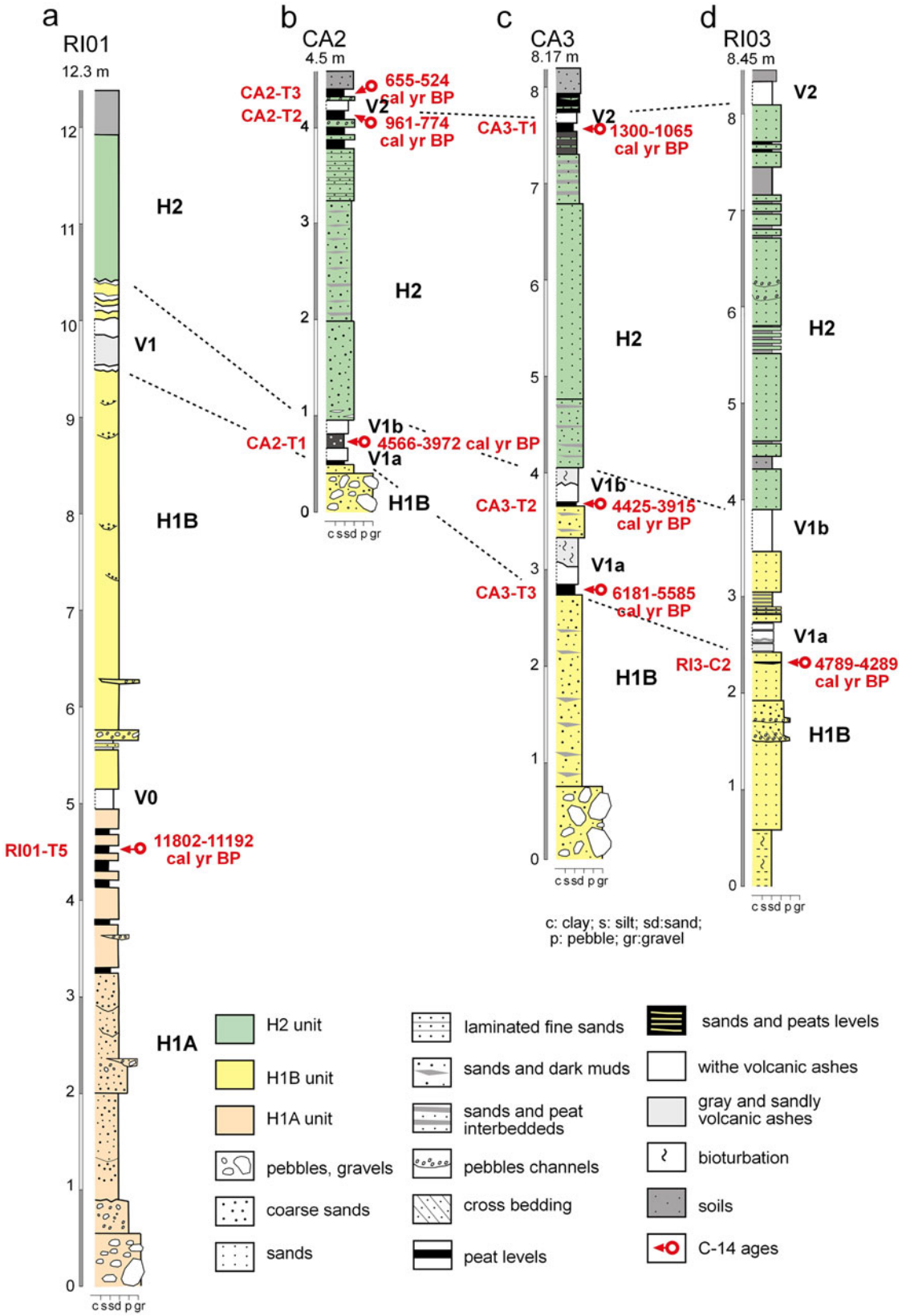

Figure 3. (color online) Representative stratigraphic profiles showing different morphosedimentary units: El Rincón (RI01) profile, with the chronostratigraphic location of the V0 tephras (a); Las Carreras (CA2 and CA3) and El Rincón (RI03) profiles, with chronological data of V0, V1a, V1b, and V2 tephras (b, c, d).

https://doi.org/10.1017/qua.2019.78 Published online by Cambridge University Press

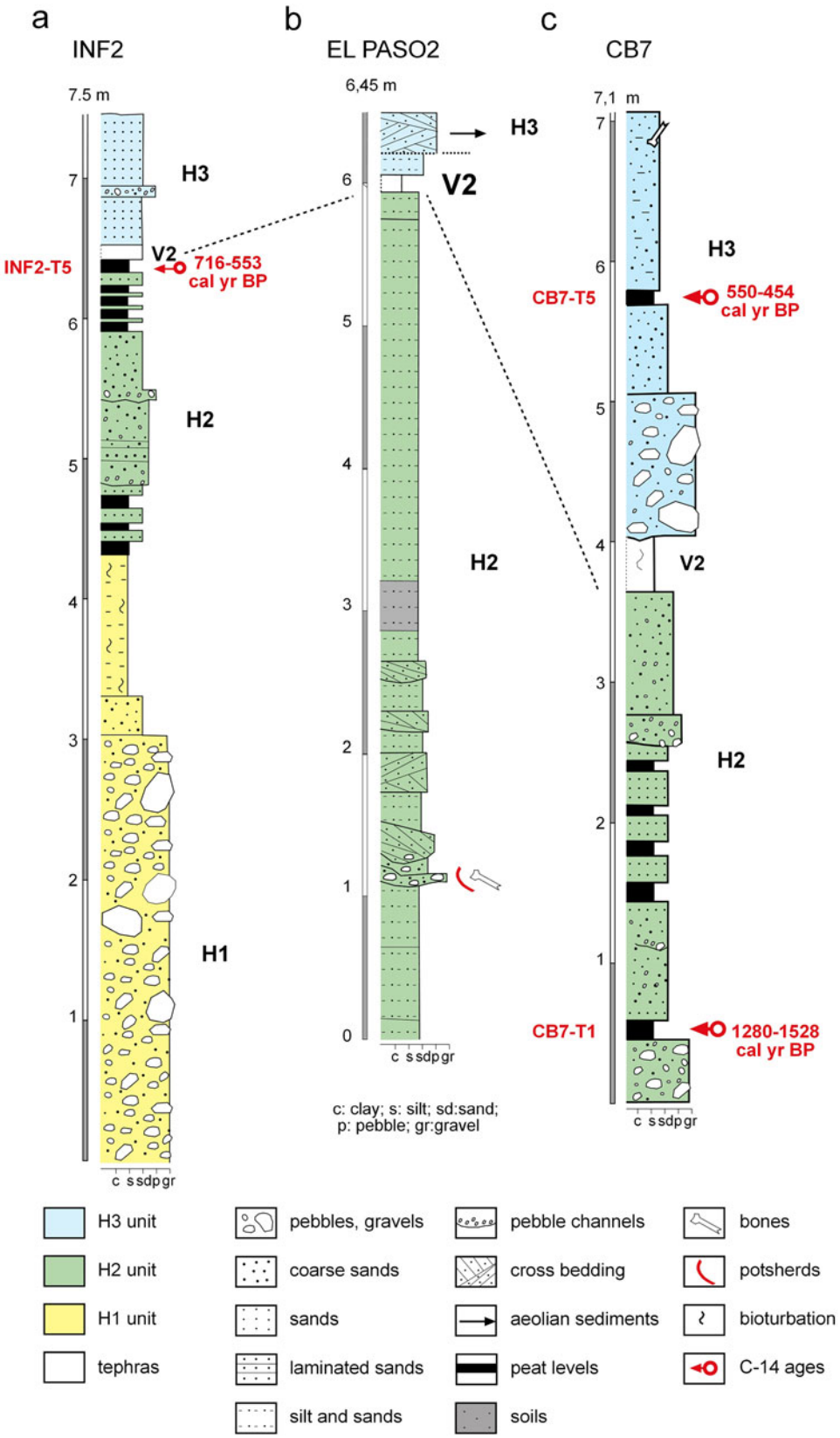

Figure 4. (color online) Stratigraphic profiles of the (a) El Infiernillo (INF2), (b) EL PASO2, and (c) Campo Blanco (CB7) showing tephra positions and chronologies in the different morphosedimentary units.

https://doi.org/10.1017/qua.2019.78 Published online by Cambridge University Press

Table 1. ^{14}C samples: u.s., underlying sediments; o.s., overlying sediments.

Profile	Sample	Relative position	^{14}C yr BP	Cal yr BP 2σ	Laboratory code	Dated material
Ri01	Ri01-T5	V0 u.s.	9980 ± 100	11,802–11,192	LP-3427	Peat
CA2	CA2-T3	V2 o.s.	630 ± 50	655–524	LP-3377	Peat
	CA2-T2	V2 u.s.	1020 ± 50	961–774	LP-3373	Peat
	CA2-T1	V1b u.s. V1a o.s.	3900 ± 100	4566–3972	LP-3375	Peat
CA3	CA3-T1	V2 u.s.	1320 ± 60	1300–1065	LP-3342	Peat
	CA3-T2	V1b u.s.	3840 ± 90	4425–3915	LP-3352	Peat
	CA3-T3	V1a u.s.	5110 ± 130	6181–5585	LP-3380	Peat
Ri03	Ri03-C2	V1 u.s.	4043 ± 50	4789–4289	D-AMS019331	Charcoal
Inf2	Inf2-T5	V2 u.s.	720 ± 50	716–553	LP-3576	Peat
CB7	CB7-T5	V2 u.s.	500 ± 40	550–454	LP-3572	Peat
	CB7-T1	V2 o.s.	1520 ± 70	1280–1528	LP-3565	Peat

marker for the transition between H1A and H1B accumulations (Figs. 2a, 3a). They are frequently visible in the bottom area of Las Carreras, El Rincón (Fig. 5a), the quarries exploited close to Tafí del Valle village (Fig. 5b), and the Carapunco and La Bolsa areas (Tafí valley). These tephras have a coarse ash texture and a high amount of biotite. Radiocarbon ages were obtained at El Rincón (RI01, Fig. 3a), on a 12-m-thick outcrop, where V0 tephra is located 5 m from its base (Fig. 3a). There are several peat layers under the ash level, the youngest dated to 11,802–11,192 cal yr BP (sample RI01-T5; Fig. 5a, Table 1). Accordingly, this tephra layer is younger than these ages (Fig. 6a). The tephra V0 was named *El Rincón ash* given the relevance of the information provided by the RI01 profile.

Previous works identified in the study area one single Middle Holocene tephra that was dated from underlying peats to after 4290±40 ^{14}C yr BP (4955–4618 cal yr BP) by Fernández-Turiel et al. (2012, 2013) and later to after 3763 ± 36 ^{14}C yr BP (4228–3927 cal yr BP) by Sampietro-Vattuone and Peña-Monné (2016). However, during geomorphological mapping and field survey, two different tephras related to the top of the H1 morphostratigraphic unit were observed in several profiles. The two identified tephras were named V1a (*Carreras 1a ash*) and V1b (*Carreras 1b ash*), and the representative profile is the CA2 section in Figure 3b. The V1a and V1b tephras were much easier to locate and distinguish than the other tephras. However, they are virtually impossible to differentiate in the field, unless they are in the same profile. While recording V1a and V1b tephras, we found catena sequences across alluvial fans where the ashes lie on top of the outcrops at the apex of the alluvial fan (Figs. 2b, 5c) and in the middle section of the outcrops recorded in the middle-low fan area (Fig. 5d). The longitudinal profiles recorded, as described in the methodology, allowed us to understand the evolution of the landforms, reinforce the value of the tephras as sedimentary, chronological, and evolutionary indicators and differentiate between H1 and H2 units when they overlap (CA2 and CA3 profiles in Fig. 3b and c, 5d). In general, V1a and V1b tephras indicate the limit between the Middle and Late Holocene, coinciding with a change in the geomorphological dynamics of the region, because the incision period separating H1 and H2 accumulation phases was just starting when the tephras fell (Sampietro-Vattuone and Peña-Monné, 2016) on top of H1B accumulations, filling shallow incisions (Fig. 2b).

As in some cases the outcrops of V1a and V1b developed interbedded peats (Fig. 5d), it was possible to make radiocarbon dating in the intermediate organic matter layers (Fig. 3b and c). In V1a, ages are later than 4789–4289 cal yr BP and earlier than 3830–3470 cal BP, while V1b tephra was dated later than 3830–3470 cal yr BP (Table 1; Figs. 3b and c, 6b). The estimated age of V1b tephra is younger than that of H2 unit, with H2 accumulation starting earlier than 2760–2188 cal yr BP, which is the radiocarbon dating of a paleosoil (s1; Fig. 2a and b) interbedded in the lower section of H2 (Sampietro-Vattuone and Peña-Monné, 2016; Peña Monné and Sampietro Vattuone, 2018c). Figure 6 offers a graphical synthesis of all available chronological data related to V1a and V1b tephras, demonstrating the existence of two eruptions very close in time and very similar in composition (see "Physicochemical characterization" section).

Finally, thin tephra layers related to the H3 morphostratigraphic units were observed in 48 profiles (i.e., Fig. 5e and f), in some cases overlying archaeological materials of the Late Period (Fig. 4b). Despite its similar compositional and macroscopic features, two different tephras were recognized, as they were dated in several outcrops (Figs. 4, 6c; Table 1). Considering only radiocarbon evidence from the CA2 profile (Fig. 4), it is possible to establish that V2 tephra is older than 991–774 cal yr BP and younger than 655–624 cal yr BP (Fig. 6c). However, other radiocarbon information from Inf2-T5 suggests that V2a tephras occurred after 716–553 cal yr BP (Figs. 4, 6c; Table 1). Moreover, the V2b tephras are lying above the paleosoil (*s2*) dated to 497–468 cal yr BP (Sayago et al., 2012) and 490–333 cal yr BP at El Paso 2 (Sampietro-Vattuone et al., 2018a). There is also another V2 sample interbedded in an H3 unit at El Paso 3. This unit was estimated to be younger than 600 yr BP (Fig. 6c)

https://doi.org/10.1017/qua.2019.78 Published online by Cambridge University Press

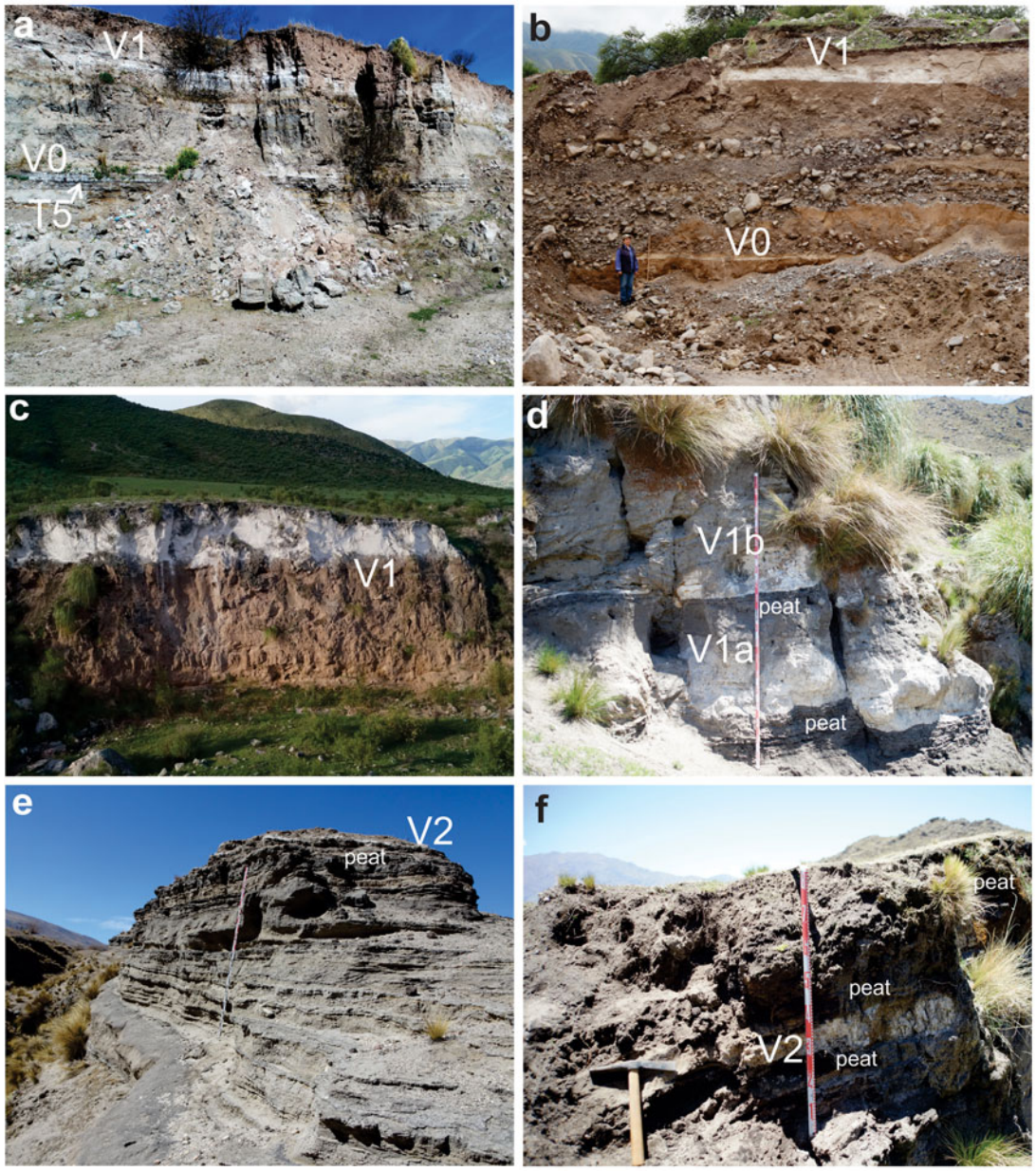

Figure 5. (color online) (a) RI01 profile showing V0 and V1 tephra positions and dated peat levels, El Rincón–Tafí valley (see Fig. 3a). (b) Profile from the quarries of La Costa (Tafí valley) showing V0 and V1 tephra levels. (c) V1 tephra from the top of an H1B unit in Tafí valley. (d) Lower section of CA2 profile showing V1a and V1b tephras with an interbedded peat in the Muñoz River, Tafí valley (see Fig. 3b). (e) INF2 profile showing V2 teprha lying over a peat level, El Infiernillo (Tafí–Santa María valleys water divide; see Fig. 4a). (f) Upper section of CA3 profile showing V2 position in the Muñoz River, Tafí valley (see Fig. 3b).

according to the evolutionary model of Sampietro-Vattuone and Peña-Monné (2016) and Peña Monné and Sampietro Vattuone (2018c). All this evidence points to the existence of two upper Holocene tephras named V2a (*Carreras 2 ash*) and V2b (*El Paso 3 ash*) (Fig. 6c).

Several features associated with the tephras, especially V1a and V1b, were also recorded in order to have a better outcrop characterization. In many cases, the thickness of each tephra could vary from a few centimeters to more than 8 m (Fig. 7a). Besides their thickness and position (Figs. 5c and d, 7a), some tephras show laminar structures at their base, followed by massive, thick deposits (Fig. 7b). In other cases, when exposed on the surface as mantles, they later developed different and distinctive erosive features such as yardangs (Fig. 7c) and taffonis and crusts in vertical exposures (Fig. 7d). There are also bioturbations represented by roots, worms, and rodent galleries filled with ashes (Fig. 7e–g). Some deposits show interbedded sand facies (Fig. 7h) and oxides, the latter normally associated with peat formations.

Physicochemical characterization

The mineralogical, textural, and geochemical features (Supplementary Table 2) of the five tephras recognized in the Tafí and

https://doi.org/10.1017/qua.2019.78 Published online by Cambridge University Press

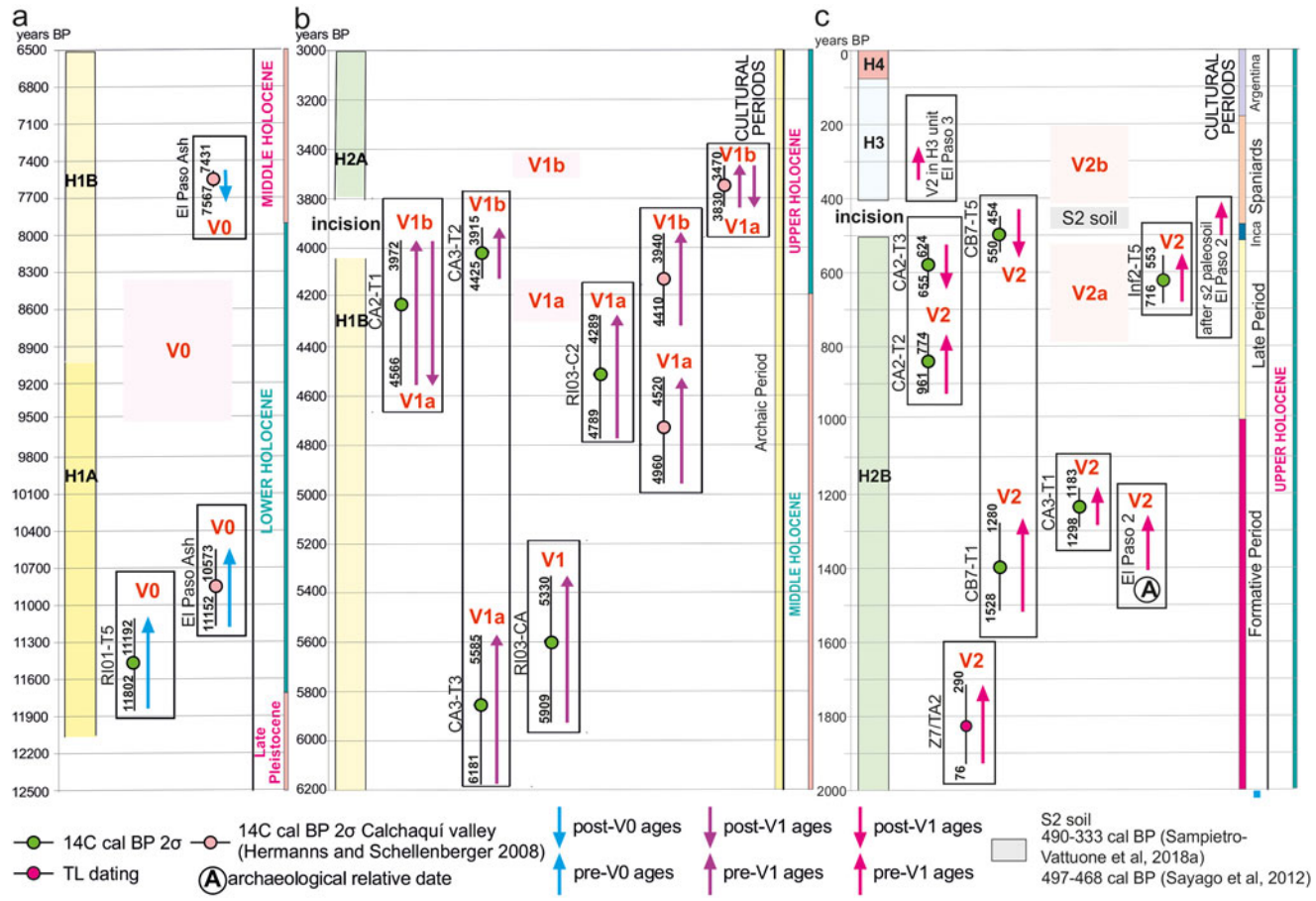

Figure 6. (color online) Synthesis of available chronological data and relative position of tephras showing the most probable sedimentation time and the reconstruction of the different events: V0 tephra (a), V1a and V1b events (b), V2a and V2b events (c).

Santa María valleys are described in the following paragraphs. Because V1a-V1b and V2a-V2b pairs are impossible to differentiate by their mineralogy, glass shard-pumice morphology, or geochemistry, both pairs are described together.

The V0 tephra is light brown and composed mainly of pumice particles and glass shards (~70%) and, to a lesser extent, crystal and lithics. The main mineral assemblage is biotite, quartz, and feldspars (mainly plagioclase) (Fig. 8a). The abundance of large crystals of biotite is an important feature that makes it possible to differentiate V0 from the other four tephras. In addition, magnetite, titanite, pyroxene, and muscovite are present as accessories. The lithics are granitic rocks, and, together with muscovite crystals, they represent a low degree of contamination of the original deposits. In V0 tephra, there is evidence of an incipient edaphization process such as the presence of oxide patinas, silty material, and organic matter, in concordance with the bioturbation observed at outcrop scale. The V0 tephra presents different morphological types of juvenile clasts. The most abundant ones are highly vesicular, irregular to subrounded pumice particles with small spherical to subspherical vesicles (Fig. 9a) or more elongated and tubular shapes separated by thin glass walls. The high vesicular pumice particles are usually covered by fine ash particles that hinder the characterization of the vesicle morphology (Fig. 9a). Another morphological type is represented by subangular, low vesicular to dense glass shards (Fig. 9b). The fine ash fraction is composed of small glass shards with flat plate and curved morphologies (Fig. 9c) derived from the fragmentation of large, highly vesicular pumice particles. In addition, we identified a low percentage of rounded, massive, slightly prolate aggregates of fine ash (Fig. 9d).

The V1a and V1b tephras are white and composed mainly of pumice particles and glass shards (~70%) and, to a lesser extent, crystals and lithics. The main mineral assemblage is quartz, feldspars (mainly plagioclase), and biotite (Fig. 8b). Magnetite, pyroxene, and amphibole are present as accessories. Edaphization and rework processes are not evident. The main compositional difference from V0 tephra is the higher percentage of pumice and glass shards and the lower proportion of crystals and crystal fragments. As in V0 tephra, the most conspicuous particle type is the highly vesicular, irregular to subrounded pumice. However, the pumice clasts from V1a and V1b tephras are characterized by more rounded vesicle morphology separated by thick glass walls (Fig. 9e) and a better development of clasts with fluid forms related to elongated and tubular vesicles (Fig. 9f). Large, subangular, low vesicular to dense glass shards and irregular prolate aggregates of fine ash are also present. The fine ash fraction consists of small glass shards with flat plate and curved morphologies.

https://doi.org/10.1017/qua.2019.78 Published online by Cambridge University Press

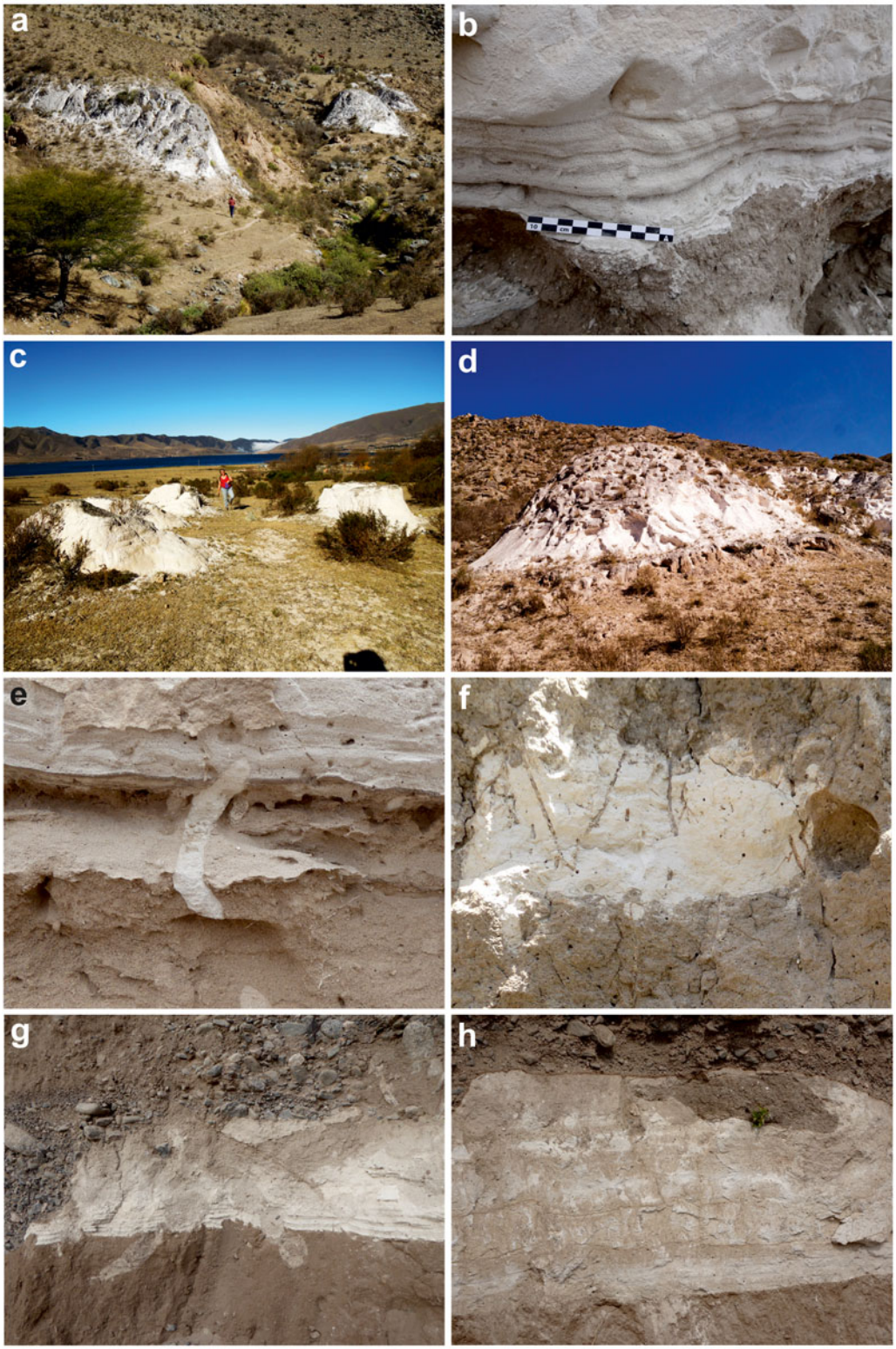

Figure 7. (color online) Features associated with tephra deposits: thick V1 deposits (a), V1 basal laminations with deformation (b), V1 tephra yardangs (c), weathered scarp (taffonis) and crust formed on exposed V1 massive tephra deposits (d), worm bioturbation on V1 tephra deposit (e), roots on V1 tephra level (f), rodent galleries crossing V1 tephra deposit (g), and V1 tephras interbedded with sand facies including oxides (h).

The V2a and V2b tephras are light gray and composed of pumice particles and glass shards, with a relatively high proportion of crystals (~30%) and lower percentages of lithics. The main mineral assemblage is amphibole, quartz, feldspars (mainly plagioclase), and biotite (Fig. 8c). The abundance of amphibole is the key feature to differentiate V2a and V2b

https://doi.org/10.1017/qua.2019.78 Published online by Cambridge University Press

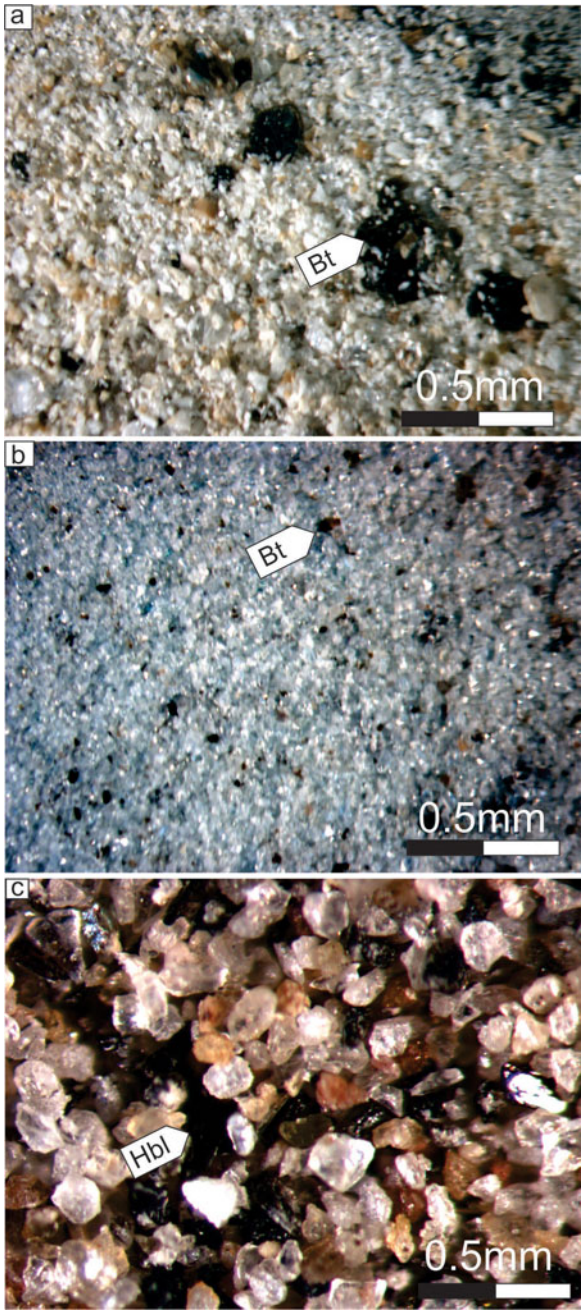

Figure 8. (color online) Photographs taken with binocular magnifying glass: abundance of large biotites (Bt) in V0 tephra (a); abundance of glass shards with respect to the crystal proportion in V1 tephra (b), and V2 tephra characterized by the high content of hornblende (Hbl) (c).

tephras from the other three tephras. Clinopiroxene, magnetite, apatite, muscovite, and rutile are present as accessories. The V2a and V2b tephras present similar types of juvenile components in terms of morphology and size. However, the most relevant feature of these tephras is the occurrence of irregular, highly vesicular pumice with complex vesicle shapes (Fig. 9g) and tubular pumice (Fig. 9h).

The data generated by pXRF are not suitable for classical geochemical classifications like the Total Alkali Silica (TAS) diagram (e.g., Le Bas et al., 1986) because some elements such as Na are not measured. However, Sr/Rb versus K/Sr ratios are essentially controlled by feldspar proportion and thus reflect approximately the igneous rock type (Sola et al., 2016). In this sense, Figure 10a shows the trace element ratios measured in our samples (Sr/Rb; K/Sr) compared with a database of volcanic rocks of the Central Andes (Mamani et al., 2010). Our geochemical data, along with the mineralogy of each ash level, indicate that V0, V1a, and V1b are probably rhyolitic in composition, whereas V2a and V2b are probably more dacitic in composition. This inference is consistent with the mineral assembly previously described. In addition, scatter plots combining trace elements with contrasting behavior, such as Rb-Sr or Zr- Sr, were used to identify the geochemical pattern for each tephra (Fig. 10b). The V1a and V1b tephras are characterized by high Rb content (>200 ppm) and low Sr content (<100 ppm). In contrast, V0, V2a, and V2b have low Rb content (<200 ppm) but can be differentiated by their Sr content: V0 < 300 ppm and V2a and V2b >300 ppm. In addition, V1a and V1b have lower Zr content (<100 ppm) than V0, V2a, and V2b (between 100 and 250 ppm).

DISCUSSION

Nature and reliability of the tephras for tephrochronology studies

The studied tephras in the Tafí and Santa María valleys show different degrees of reworking. Although some of them can be interpreted as primary fallout deposits, abrupt changes in the tephra thicknesses through adjacent outcrops and incipient mixing with epiclastic material provide evidence that reworking occurred in most cases. The laminar structures at the base of some tephras, particularly V1a, are inferred as primary features related to eruptive column heights instability (e.g., Fernández-Turiel et al., 2019). Remobilization syneruptive and/or early posteruptive (tens of years after eruption) of primary tephras is a well-recorded process worldwide, especially in desert regions such as Patagonia (e.g., Wilson et al., 2011; Forte et al., 2018). The relative compositional homogeneity revealed by petrographic and geochemical data, along with the good preservation of the primary textural features of the studied tephras, suggests that the reworking was very localized and near contemporaneous with the primary fallout event. For this reason, the term "tephra" is maintained for the designation of the pyroclastic levels studied, as in other case studies (e.g., Froese et al., 2006). We consider that the primary fall and the final disposition after the reworking of the studied tephras probably occurred over a period of tens of years. Therefore, the studied tephras are not reliable for very high-resolution tephrochronological studies, but they may still provide useful chronostratigraphic information depending on the expected temporal resolution (Lowe, 2011), such as for identification and correlation of the main Holocene aggradation units in the study

https://doi.org/10.1017/qua.2019.78 Published online by Cambridge University Press

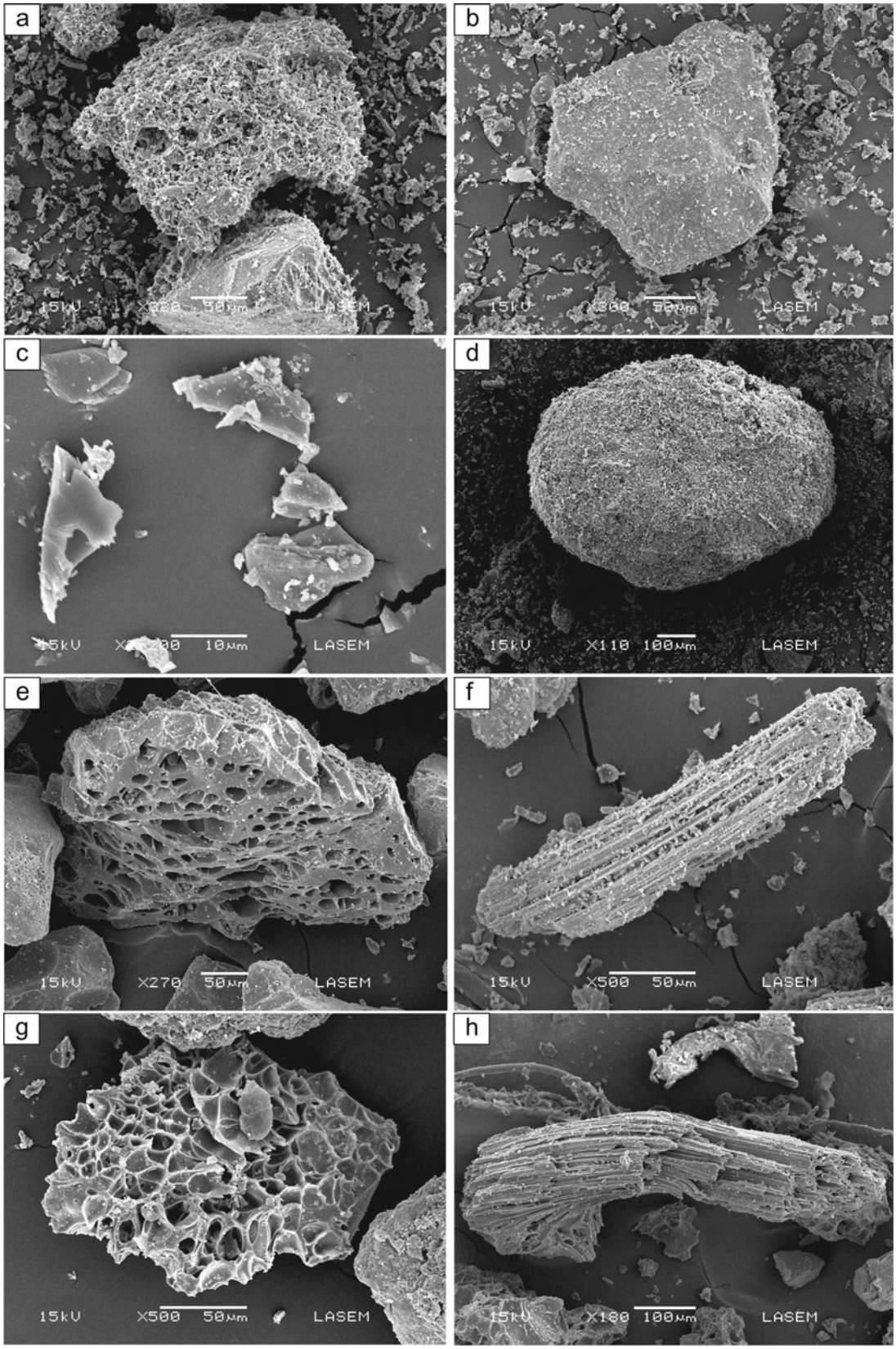

Figure 9. Scanning electron microscopy images: highly vesicular irregular to subrounded pumice particles in V0 tephra (a), subangular low vesicular to dense glass shards in V0 tephra (b), glass shard with flat plate and curved morphologies from V0 tephra (c), aggregates of fine ash from the V0 tephra (d), pumice clasts from V1 tephra characterized by rounded vesicle morphology separated by thick glass walls (e), pumice clasts from V1 tephra with fluid forms and elongated to tubular vesicles (f), highly vesicular pumice with complex vesicle shapes from V2 tephra (g), and tubular pumice in V2 tephra (h).

https://doi.org/10.1017/qua.2019.78 Published online by Cambridge University Press

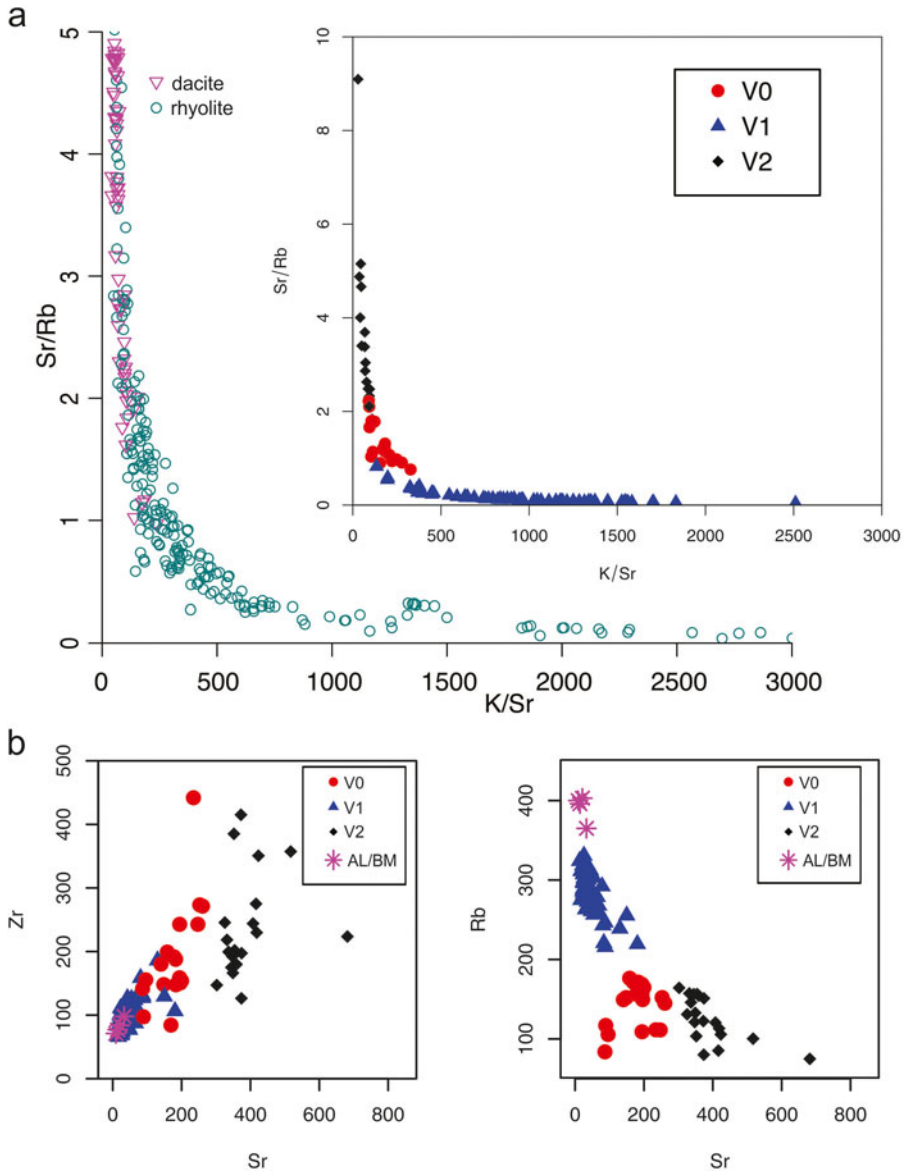

Figure 10. (color online) (a) Relative geochemical classification using Sr/Rb versus K/Sr diagram proposed by Sola et al. (2016), with dacites and rhyolites of the Central Andes compiled by Mamaní et al. (2010) and the samples analyzed in this work. (b) AL/BM: geochemical data of the Alemanía and Buey Muerto ashes taken from Hermanns et al. (2008).

area (e.g., Peña Monné and Sampietro Vattuone, 2016b; Sampietro-Vattuone and Peña-Monné, 2016).

Another finding from our research is the existence of tephras that are very similar in composition and relatively close in time. These compositional similarities suggest that they come from the same eruptive center. The occurrence of eruptions similar in composition throughout the evolution of one single eruptive center is not extremely strange in the Central Andes (e.g., Folkes et al., 2011). The physicochemical characterization presented in this article does not have enough resolution to identify the fingerprints of these kinds of geochemically homogeneous eruptions. Thus, V1a-V1b and V2a-V2b tephras are not useful for high-resolution tephrochronological studies. However, tephras related to the same volcano accumulated as stratigraphically contiguous tephra layers over longer periods, from some years to millennia, are still able to provide chronostratigraphic information (Lowe, 2011). In this sense, each pair of tephras (V1a-V1b, V2a-V2b) can be understood as "composite" isochrons defined by a pair of maximum and minimum time lines (Lowe, 2011).

Tephrostratigraphy of Tafí and Santa María valleys

Although the chronological value of the tephras in reconstructing geomorphological and geoarchaeological evolutionary processes in the study area was recognized and reported by Peña Monné and Sampietro Vattuone (2016b) and Sampietro-Vattuone and Peña-Monné (2016), this is the first study of the complete set of Holocene tephras from Tafí and Santa María valleys. The morphostratigraphic analysis and new geochronological data presented here have allowed us to identify five temporally well-defined Holocene

https://doi.org/10.1017/qua.2019.78 Published online by Cambridge University Press

tephras, some of which are mentioned for the first time in the study area. Thus, these tephras had never been described, chronologically situated, placed into their morphosedimentary context, or physicochemically characterized before.

V0 is the oldest Holocene tephra in the study area. Our results indicate that V0 was deposited after 11,802–11,192 cal yr BP and before 4789–4289 cal yr BP (maximum age for the overlaying V1a tephra). Thus, V0 is probably equivalent to "El Paso ash," previously characterized by Hermanns and Schellenberger (2008), improving our chronological frame to after 11,152–10,573 cal yr BP and before 7567–7431 cal yr BP (Fig. 5a). This chronological frame also suggests that V0 is equivalent to the "CdP1 unit" (Cueros de Purulla sequence), defined by Fernández-Turiel et al. (2019) in the northern sector of the Calchaquí valley. The physicochemical characteristics of V0 are roughly consistent with this interpretation. Our geochronological data show that V1a and V1b tephras probably represent the same tephras assigned by Fernández-Turiel et al. (2019) to the Holocene Cerro Blanco caldera-forming eruption (Fernández-Turiel et al. 2012, 2013; Báez, 2014; Báez et al., 2015). However, according to our chronological and morphosedimentary data, V1a and V1b represent two temporally well-defined, independent eruptions. In addition, V1a (*Carreras 1a ash*) and V1b (*Carreras 1b ash*) tephra layers represent the previously defined Buey Muerto and Alemanía ashes (Hermanns et al., 2000, 2006; Hermanns and Schellenberger, 2008) because they cannot be differentiated by analytical procedures either and are contemporaneous with our V1a and V1b tephras. We agree with the interpretation of Hermanns and Schellenberger (2008) that tephra reworking is unlikely to have occurred over the long period of time (~1000 yr) that separates both tephra layers. The lack of evidence of significant contamination in V1b tephra is also consistent with the inference that V1a and V1b tephras (Buey Muerto and Alemania ashes according to Hermanns and Schellenberger [2008]) represent two individual eruptions rather than long-lasting (hundreds of years) reworking processes.

Finally, the V2a and V2b tephras (*Carreras 2 ash* and *El Paso 3 ash* tephras) have been characterized and dated for the first time in the study area, and they represent the youngest large volcanic eruptions (younger than 800 yr BP) in this sector of the Central Andes. Fernandez-Turiel et al. (2019) have identified a new tephra in the Fiambalá valley (BdF unit of the Fiambalá sequence) and suggested that it can be correlated with the youngest tephras of the Tafí valley (V2a and V2b). Yet, high-resolution tephrochronological studies are necessary to confirm these preliminary correlations.

Volcanological implications

Considering that the preservation potential of fallout deposits hundreds of kilometers away from their source is only related to large volcanic eruptions (VEI >6), the occurrence of the five tephras presented in this work has important implications in volcanic hazard and risk assessment in northwestern Argentina. At least five major eruptions affected the Tafí and Santa María valleys in the last 10,000 yr; therefore, this area should be considered a vulnerable zone in terms of tephra fall.

The source of the V0 tephra is unknown; however, explosive volcanic activity of rhyolitic composition during the Holocene along the southern edge of the Central Volcanic Zone was very scarce and mainly concentrated in the back-arc region (Guzmán et al., 2014; Grosse et al., 2017; Petrinovic et al., 2017). Few volcanic centers with Quaternary explosive rhyolitic activity were identified in this sector of the Central Andes, and they usually have relatively homogeneous geochemical compositions. Two examples of these centers are Cerro Blanco Volcanic Complex (Báez et al., 2015 and references therein) and Cueros de Purulla volcano (Báez, 2014) (Fig. 1). Fernández-Turiel et al. (2019) proposed that "El Paso ash" (Hermanns and Schellemberger, 2008) and equivalent units were ejected from the Cueros de Purulla volcano. This correlation is weak, as it is based only on the compositional similarities with the proximal fallout deposits of the Cuero de Purulla volcano and "El Paso ash," and no geochronological data are available for the Cuero de Purulla volcano.

To date, the only tephra in the study area that has correlated well with a specific volcanic center is the middle Holocene tephra related to the Cerro Blanco eruption (Fernández-Turiel et al., 2019). However, the results presented in this article point to two eruptions of the Cerro Blanco Volcanic Complex during Holocene times (V1a and V1b tephras).

The source of the V2a and V2b tephras is unknown, but their amphibole-rich and more "dacitic" composition suggests that they are related to some volcanic center located along the main arc with highly explosive activity during the Holocene, like the Nevado Tres Cruces (Gardeweg et al., 2000), as previously proposed by Fernández-Turiel et al. (2019).

CONCLUSIONS

Five temporally well-defined Holocene tephra layers were identified in Tafí and Santa María valleys. The morphostratigraphic position of these tephras, together with radiocarbon data, contributed to establishing a valuable chronological framework. The oldest layer, named *El Rincón ash* (V0), is younger than 11,802–11,192 cal yr BP and older than 7567–7431 cal yr BP. Two younger tephras named *Carreras 1a ash* (V1a) and *Carreras 1b ash* (V1b) were identified. They are equal in their composition and were dated between 4789–4289 and 3830–3470 cal yr BP (V1a) and between 3830–3470 and 2760–2188 cal yr BP (V1b). Finally, two very young (upper Holocene) tephras named *Carreras 2 ash* (V2a), dated between 991–774 and 655–624 cal yr BP, and *El Paso 3 ash* (V2b), dated later than 497–468 cal yr BP, were identified in the study area.

Geochemical and mineralogical data allowed us to know that V0, V1a, and V1b tephras are rhyolitic in composition, whereas V2a and V2b are dacitic. Considering that in this sector of the Central Andes the occurrence of Quaternary explosive rhyolitic eruptions is restricted to the Puna region, the

https://doi.org/10.1017/qua.2019.78 Published online by Cambridge University Press

back-arc region was the most active area providing tephras to the region during the Holocene.

The new data presented in this work have important implications in volcanic hazard and risk assessment in northwestern Argentina. In this sense, we highlight the identification of one unknown Middle Holocene (V1b) and two other very young (<800 yr BP) tephra layers (V2a and V2b) in the study area.

ACKNOWLEDGMENTS

This work is a contribution of the "Primeros Pobladores del Valle del Ebro" research group (Government of Aragon and European Social Fund) and fits within the research scope of IUCA (Environmental Sciences Institute of the University of Zaragoza). This research was supported by Universidad Nacional de Tucumán (PIUNT G629), CONICET (PIP 837), Universidad Nacional de Salta (CIUNSa Type B - N° 2618), and Agencia Nacional de Promoción Científica y Tecnológica (PICT 2016-1359).

SUPPLEMENTARY MATERIAL

The supplementary material for this article can be found at https://doi.org/10.1017/qua.2019.78.

REFERENCES

Báez, W., 2014. *Estratigrafía volcánica, estilos eruptivos y evolución del Complejo Volcánico Cerro Blanco, Puna Austral*. PhD dissertation, Universidad Nacional de Salta, Salta, Argentina.

Báez, W., Arnosio, M., Chiodi, A., Ortiz Yañes, A., Viramonte, J.G., Bustos, E., Giordano, G., López, J.F., 2015. Estratigrafía y evolución del Complejo Volcánico Cerro Blanco, Puna Austral, Argentina. *Revista Mexicana de Ciencias Geológicas* 32, 29–49.

Báez, W.A., Chiodi, A., Bustos, E., Arnosio, M., Viramonte, J.G., Giordano, G., Alfaro Ortega, B., 2017. Mecanismos de emplazamiento y detrucción de los domos lávicos asociados a la caldera del Cerro Blanco, Puna Austral. *Revista de la Asociación geológica Argentina* 74(2), 223–238.

Bertin, D., Baez, W., Caffe, P., Elissondo, M., Lindsay, J., 2018. Active volcanoes of the Central Andes: an Argentinian perspective. Actas del XV Congreso Geológico Chileno. VOLC-1, 958.

Bossi, G.E., Georgieff, S.M., Gavriloff, I.J.C., Ibañez, L.M., Muruaga, C.M., 2001. Cenozoic evolution of the intramontane Santa Maria basin, Pampean Ranges, northwestern Argentina. *Journal of South American Earth Science* 14, 725–734.

Collantes, M.M., 2001. *Paleogeomorfología y Geología del Cuaternario de la cuenca del río Tafí, Depto*. Tafí del Valle, Prov. de Tucumán, Argentina. PhD dissertation, Universidad Nacional de Salta, Salta, Argentina.

Collantes, M.M., 2007. Evolución morfogenética y paleoambiental del valle de Tafí durante el Pleistoceno tardío y Holoceno. In: Arenas, P., Manasse, B., Noli, E. (Eds.), *Paisajes y procesos sociales en Tafí del Valle*. Magna Publicaciones, Tucumán, Argentina, pp. 261–288.

Fernández-Turiel, J.L., Saavedra, J., Pérez-Torrado, F.J., Rodríguez-González, A., Alias, G., Rodríguez-Fernández, D., 2012. Los depósitos de ceniza volcánica del Pleistoceno Superior-Holoceno de la región de Tafí del Valle-Cafayate, noroeste de Argentina. Geo-Temas 13, CD 07-279 P.

Fernández-Turiel, J.L., Saavedra, J., Pérez-Torrado, F.J., Rodríguez-González, A., Carracedo, J.C., Lobo, A., Rejas, M., *et al*., 2015. The ash deposits of the 4200 BP Cerro Blanco eruption: the largest Holocene eruption of the Central Andes. *Geophysical Research Abstracts* 17, 3392.

Fernández-Turiel, J.L., Saavedra, J., Perez-Torrado, F.J., Rodríguez-González, A., Carracedo, J.C., Osterrieth, M., Carrizo, J.I., Esteban, G., 2013. The largest Holocene eruption of the Central Andes found. American Geophysical Union, Fall Meeting 2013, abstract V13D-2639.

Fernández-Turiel, J.L., Perez-Torrado, F.J., Rodríguez González, A., Saavedra, J., Carracedo, J.C., Rejas, M., Lobo, A., *et al*., 2019. The large eruption 4.2 ka cal BP in Cerro Blanco, Central Volcanic Zone, Andes: insights to the Holocene eruptive deposits in the Southern Puna and adjacent regions. *Estudios Geológicos* 75, e088.

Folkes, C.B., de Silva, S.L., Wright, H.M., Cas, R.A., 2011. Geochemical homogeneity of a long-lived, large silicic system; evidence from the Cerro Galán caldera, NW Argentina. *Bulletin of Volcanology* 73, 1455–1486.

Forte, P., Dominguez, L., Bonadonna, C., Gregg, C.E., Bran, D., Bird, D., Castro, J.M., 2018. Ash resuspension related to the 2011–2012 Cordón Caulle eruption, Chile, in a rural community of Patagonia, Argentina. *Journal of Volcanology and Geothermal Research* 350, 18–32.

Froese, D.G., Zazula, G.D., Reyes, A.V., 2006. Seasonality of the late Pleistocene Dawson tephra and exceptional preservation of a buried riparian surface in central Yukon Territory, Canada. *Quaternary Science Reviews* 25, 1542–1551.

Galván, A.F., 1981. Descripción geológica de la Hoja 10e, Cafayate, Provincias de Tucumán, Salta y Catamarca. Escala 1:200.000. Servicio Geológico Nacional, Boletín 177. Servicio Geológico Nacional, Buenos Aires, Argentina.

Gardeweg, M., Clavero, J., Mpodozis, C., Pérez, C., Villeneuve, M., 2000. El Macizo Tres Cruces: un complejo volcánico longevo y potencialmente activo en la Alta Cordillera de Copiapó, Chile. In: *IX Congreso Geológico Chileno*, Puerto Varas, Chile, pp. 291–295.

Gardeweg, M.C., Sparks, R.S.J., Matthews, S.J., 1998. Evolution of Lascar Volcano, northern Chile. *Journal of the Geological Society* 155, 89–104.

Garreaud, R.D., Vuille, M., Compagnucci, R., Marengo, J., 2009. Present-day South American climate. *Palaeogeography, Palaeoclimatology, Palaeoecology* 281, 180–195.

González, O.E., 1997. Geología de La Angostura, valle de Tafí, Tucuman. In: *XIV Congreso Geológico Argentino*, Salta, Argentina, pp. 283–286.

Grosse, P., Guzmán, S., Petrinovic, I., 2017. Volcanes compuestos cenozoicos del Noroeste Argentino. In: Muruaga, C., Grosse, P. (Eds.), *Ciencias de la Tierra y Recursos Naturales del NOA*. Asociación Geológica Argentina, Tucumán, Argentina, pp. 484–517.

Grosse, P., Orihashi, Y., Guzmán, S.R., Sumino, H., Nagao, K., 2018. Eruptive history of Incahuasi, Falso Azufre and El Cóndor Quaternary composite volcanoes, southern Central Andes. *Bulletin of Volcanology* 80, 44.

Guzmán, S., Grosse, P., Montero-López, C., Hongn, F., Pilger, R., Petrinovic, I., Seggiaro, R., Aramayo, A., 2014. Spatial–temporal distribution of explosive volcanism in the 25–28° S segment of the Andean Central Volcanic Zone. *Tectonophysics* 636, 170–189.

Hermanns, R.L., Folguera, A., Penna, I., Fauqué, L., Niedermann, S., 2011. Landslide dams in the Central Andes of

Argentina (Northern Patagonia and the Argentine Northwest). In: Evans, S.G., Hermanns, R.L., Scarascia Mugnozza, G., Strom, A. (Eds.), *Natural and Artificial Rockslide Dams*. Lecture Notes in Earth Sciences, Vol. 133. Springer, Berlin, pp. 147–176.

Hermanns, R.L., Niedermann, S., Villanueva García, A., Schellenberger, A., 2006. Rock avalanching in the NW Argentine Andes as result of complex interactions of lithologic, structural and topographic boundary conditions, climate change and active tectonics. In: Evans, S.G., Scarascia-Mugnozza, G., Strom, A., Hermanns, R.L. (Eds.), *Massive Rock Slope Failure: New Models for Hazard Assessment*. NATO Science Series. Kluwer, Dordrecht, the Netherlands, pp. 539–569.

Hermanns, R.L., Schellenberger, A., 2008. Quaternary tephrochronology helps define conditioning factors and triggering mechanisms of rock avalanches in NW Argentina. *Quaternary International* 178, 261–275.

Hermanns, R.L., Trauth, M.H., Niedermann, S., McWilliams, M., Strecker, M.R., 2000. Tephrochronologic constraints on temporal distribution of large landslides in Northwest Argentina. *Journal of Geology* 108, 35–52.

Kay, S.M., Coira, B.L., 2009. Shallowing and steepening subduction zones, continental lithospheric loss, magmatism, and crustalflow under the Central Andean Altiplano-Puna Plateau. In: Kay, S.M., Ramos, V.A., Dickinson, W.R. (Eds.), *Backbone of the Americas: Shallow Subduction, Plateau Uplift, and Ridge and Terrane Collision*. Memoir 204. Geological Society of America, Boulder, CO, p. 229.

Knight, R.D., Kjarsgaard, B.A., Plourde, A.P., Moroz, M., 2013. Portable XRF Spectrometry of Reference Materials with Respect to Precision, Accuracy, Instrument Drift, Dwell Time Optimization, and Calibration. Geological Survey of Canada Open File 7358. Geological Survey of Canada, Ottawa.

Le Bas, M.J., Le Maitre, R.W., Streckeisen, A., Zanettin, B., 1986. A chemical classification of volcanic rocks based on the total alkali–silica diagram. *Journal of Petrology* 27, 745–750.

Lowe, D.J., 2011. Tephrochronology and its application: a review. *Quaternary Geochronology* 6, 107–153.

Mamani, M., Wörner, G., Sempere, T., 2010. Geochemical variations in igneous rocks of the Central Andean orocline (13°S to 18°S): tracing crustal thickening and magma generation through time and space. *Geological Society of America Bulletin* 122, 162–182.

May, J.H., Zech, R., Schellenberger, A., Kull, C., Veit, H., 2011. Quaternary environmental and climate changes in the Central Andes. In: Salfity, J.A., Marquillas, R.A. (Eds.), *Cenozoic Geology of the Central Andes of Argentina*. SCS, Salta, Argentina, pp. 247–263.

Peña Monné, J.L., 1997. *Cartografía geomorfológica*. Geoforma Ediciones, Logroño, Spain.

Peña-Monné, J.L., Sampietro-Vattuone, M.M., 2016a. Geomorphology of the alluvial fans in Colalao del Valle-Quilmes area (Santa María Valley, Tucumán Province, Argentina). *Journal of Maps* 12, 460–465.

Peña Monné, J.L., Sampietro Vattuone, M.M., 2016b. La secuencia paleoambiental holocena de la vertiente oriental de Loma Pelada (valle de Tafí, Noroeste Argentino): cambios climáticos y acción humana. In: Sampietro Vattuone, M.M., Peña Monné, J.L. (Eds.), *Geoarqueología de los Valles Calchaquíes*. Laboratorio de Geoarqueología, Tucumán, Argentina, pp. 23–63.

Peña Monné, J.L., Sampietro Vattuone, M.M., 2018a. Evolución geomorfológica de los conos aluviales de los ríos Pichao y Managua (valle de Santa María, prov. De Tucumán, Argentina). In: Blanco, R., Castillo, F., Costa, M., Horacio, J., Valcárcel, M. (Eds.), *Xeomorfoloxía e paisaxes xeográficas: catro décadas de investigación e ensino*. Homenaxe a Augusto Pérez Alberti. Universidad de Santiago de Compostela, Santiago de Compostela, Spain, pp. 429–447.

Peña-Monné, J.L., Sampietro-Vattuone, M.M., 2018b. Fluvial and aeolian dynamics of the Santa María River in the Cafayate depression (Salta Province, NW Argentina). *Journal of Maps* 14, 567–575.

Peña Monné, J.L., Sampietro Vattuone, M.M., 2018c. Paleoambientes holocenos del valle de Tafí (Noroeste Argentino) a partir de registros morfosedimentarios y geoarqueológicos. *Boletín Geológico Minero* 129, 671–691.

Peña-Monné, J.L., Sancho-Marcén, C., Sampietro-Vattuone, M.M., Rivelli, F., Rhodes, E.J., Osacar-Soriano, M.C., Rubio-Fernández, V., García-Giménez, R., 2015. Environmental change over the last millennium recorded in the Cafayate Dune field (NW Argentina). *Palaeogeography, Palaeoclimatology, Palaeoecology* 438, 352–363.

Peña Monné, J.L., Sancho Marcén, C., Sampietro Vattuone, M.M., Rivelli, F., Rhodes, E., Osácar Soriano, M.C., Rubio Fernández, V., García Giménez, R., 2016. Geomorfología y cambios ambientales en la depresión de Cafayate (Prov. de Salta, Noroeste Argentino). In: Sampietro Vattuone, M.M., Peña Monné, J.L. (Eds.), *Geoarqueología de los Valles Calchaquíes*. Laboratorio de Geoarqueología, Tucumán, Argentina, pp. 213–242.

Perea, M.C., 1995. Mapa de vegetación del Valle de Santa María, sector oriental (Tucumán, Argentina). *Lilloa* 38, 213–235.

Petrinovic, I.A., Grosse, P., Guzman, S., Caffe, P.J., 2017. Evolución del volcanismo cenozoico en la Puna argentina. In: Muruaga, C., Grosse, P. (Eds.), *Ciencias de la Tierra y Recursos Naturales del NOA*. Asociación Geológica Argentina, Tucumán, Argentina, pp. 469–483.

Ruiz Huidobro, O.J., 1972. Descripción Geológica de la hoja 11e, Santa María, Provincias de Catamarca y Tucumán. Servicio Nacional Minero Geológico, Boletín 134. Servicio Nacional Minero Geológico, Buenos Aires, Argentina.

Sampietro Vattuone, M.M., Neder, L., 2011. Quaternary landscape evolution and human occupation in Northwest Argentina. *Geological Society of London* 352, 37–47.

Sampietro-Vattuone, M.M., Peña-Monné, J.L., 2016. Geomorphological dynamic changes during the Holocene through ephemeral stream analyses from Northwest Argentina. *Catena* 147, 663–677.

Sampietro Vattuone, M.M., Peña Monné, J.L., Báez, W., Ortíz, P., Aguirre, M.G., 2016. Unidades morfosedimentarias holocenas en la quebrada de La Angostura (valle de Tafí, Noroeste de Argentina). In: Sampietro Vattuone, M.M., Peña Monné, J.L. (Eds.), *Geoarqueología de los Valles Calchaquíes*. Laboratorio de Geoarqueología, Tucumán, Argentina, pp. 3–22.

Sampietro Vattuone, M.M., Peña Monné, J.L., Maldonado, M.G., Sancho Marcén, C., Báez, W., Sola, A., 2018a. Cambios ambientales durante el Holoceno superior registrados en secuencias morfosedimentarias fluvio-eólicas del valle de Santa María (Noroeste Argentino). *Boletín Geológico Minero* 129, 647–669.

Sampietro Vattuone, M.M., Peña-Monné, J.L., Roldán, J., Maldonado, M.G., Lefebvre, M.G., Vattuone, M.A., 2018b. Human-driven geomorphological processes and soil degradation in Northwest Argentina: a geoarchaeological view. *Land Degradation & Development* 29, 3852–3865.

Sampietro-Vattuone, M.M., Peña-Monné, J.L., 2019. Geomorphology of Tafí valley (Tucumán Province, Northwest Argentina). *Journal of Maps* 15(2), 177–184.

https://doi.org/10.1017/qua.2019.78 Published online by Cambridge University Press

Sampietro Vattuone, M.M., Sola, A., Báez, W., Peña Monné, J.L., 2017. Aplicación de la correlación geoquímica de niveles cineríticos en la reconstrucción de las secuencias morfosedimentarias holocenas del valle de Tafí. In: Muruaga, C., Grosse, P. (Eds.), *Ciencias de la Tierra y Recursos Naturales del NOA*. Asociación Geológica Argentina, Tucumán, Argentina, pp. 67–72.

Sayago, J.M., Collantes, M.M., 1991. Evolución paleogeomorfológica del valle de Tafí (Tucumán, Argentina) durante el Cuaternario Superior. *Bamberger Geographische Schriften* 11, 109–124.

Sayago, J.M., Collantes, M.M., Niz, A., 2012. El umbral de resiliencia del paisaje en el proceso de desertificación de los valles preandinos de Catamarca (Argentina). *Acta Geológica Lilloana* 24, 62–79.

Sayago, J.M., Powell, J., Collantes, M.M., Neder, L., 1998. EI Cuaternario. In: Gianfrancisco, M., Puchulu, M.E., Durango de Cabrera, J., Aceñolaza, G.F. (Eds.), *Geología de Tucumán*. Colegio Graduados Ciencias Geológicas de Tucumán, Tucumán, Argentina, pp. 111–128.

Siebert, L., Simkin, T., Kimberley, P., 2010. *Volcanoes of the World*, third ed. University of California Press.

Sola, A.M., Báez, W., Bustos, E., Hernandez, R., Sampietro Vattuone, M.M., Peña Monné, J.L., Becchio, R.A., 2016. Cluster analysis using portable X ray fluorescence (pXRF) data: a fast and powerful method for regional correlation of ash fall deposits. In: Cities on Volcanoes 9, Puerto Varas, Chile, p. 1.

Strecker, M.R., 1987. *Late Cenozoic Landscape Development, the Santa María Valley, Northwest Argentina*. PhD dissertation, Cornell University, Ithaca, NY.

Toselli, A.J., Rossi de Toselli, J.N., Rapela, C.W., 1978. El basamento metamórfico de la Sierra de Quilmes, República Argentina. *Revista de la Asociación Geológica Argentina* 33, 105–121.

Trauth, M.H., Alonso, R.A., Haselton, K.R., Hermanns, R.L., Strecker, M.R., 2000. Climate change and mass movements in the NW Argentine Andes. *Earth and Planetary Science Letters* 179, 243–256.

Wilson, T.M., Cole, J.W., Stewart, C., Cronin, S.J., Johnston, D.M., 2011. Ash storms: impacts of wind-remobilised volcanic ash on rural communities and agriculture following the 1991 Hudson eruption, southern Patagonia, Chile. *Bulletin of Volcanology* 73, 223–239.

https://doi.org/10.1017/qua.2019.78 Published online by Cambridge University Press